SPANDIDOS PUBLICATIONS

ONCOLOGY LETTERS 14: 6170-6176, 2017

Artesunate inhibits proliferation and invasion of mouse hemangioendothelioma cells *in vitro* and of tumor growth *in vivo*

NING WANG[1-3], HONGXIA CHEN[1-3], YINPING TENG[1-3], XIONGHUI DING[1,3], HUAN WU[1-3] and XIANQING JIN[1-4]

[1]Ministry of Education Key Laboratory of Child Development and Disorders; [2]Key Laboratory of Pediatrics in Chongqing; [3]China International Science and Technology Cooperation Center for Child Development and Disorders; [4]Department of Neonatal Gastrointestinal Surgery Children's Hospital, Chongqing Medical University, Yuzhong, Chongqing 400014, P.R. China

Received January 23, 2016; Accepted June 9, 2017

DOI: 10.3892/ol.2017.6986

Abstract. Artesunate has been demonstrated to be a novel potential antitumor agent in numerous studies. However, its efficacy in infantile hemangioma is unknown. The aim of the present study was to investigate the role of artesunate in the control of vascular tumor biological behavior and molecular mechanism using mouse hemangioendothelioma endothelial (EOMA) cells and a nude mouse model. Cell viability, apoptosis and invasion were determined by an MTT assay, flow cytometric analysis and Transwell invasion assay, respectively. Reverse transcription-quantitative polymerase chain reaction and western blotting were utilized to examine the expression of genes and proteins. Inoculated EOMA cells were injected into the subcutaneous tissues of nude mice to observe the effect of artesunate therapy on the vascular tumor, an effect that was similar to that of pingyangmycin (PYM). It was identified that artesunate treatment (0-600 μg/ml) inhibited cell growth in a time- and dose-dependent manner. Artesunate at 300 μg/ml significantly reduced the proliferation and invasion of EOMA cells, and significantly decreased the expression of vascular endothelial growth factor (VEGF)-A, VEGFR-1, VEGFR-2 and hypoxia inducible factor-1α over time; caspase-3 was simultaneously upregulated *in vitro*. Artesunate significantly inhibited tumor growth, and the curative effect was similar to that observed with PYM *in vivo*. It was concluded that artesunate could effectively inhibit the growth of vascular tumors, and thus could be a novel drug candidate for the treatment of infantile hemangioma.

Correspondence to: Professor Xianqing Jin, Department of Neonatal Gastrointestinal Surgery Children's Hospital, Chongqing Medical University, 136 Zhongshan 2nd Road, Yuzhong, Chongqing 400014, P.R. China
E-mail: jinxianqing@yeah.net

Key words: artesunate, hemangioma, mouse hemangioendothelioma endothelial cells, hypoxia inducible factor-1α, vascular endothelial growth factor-A

Introduction

Hemangioma is a type of congenital vascular dysplasia common among infants and young children, with a high incidence rate of ~10-12% (1). The primary pathological features of hemangioma include the excessive proliferation of vascular endothelial cells and the formation of an abnormal vascular cavity (2). Kasabach-Merritt syndrome (K-MS; large hemangioma with thrombocytopenia syndrome) is a serious and life-threatening hemangioma (3-7), which is often associated with comorbid conditions such as hemangioendothelioma (8-10) or plexiform hemangioma (tufted angiomas) (11). In addition to the rapid increase in the size of the tumor, other features of the syndrome include the development of a low platelet count, microvascular disease, anemia and blood coagulation dysfunctions (12). In the present study, it was generally considered that vasculogenesis and angiogenesis are involved in the formation of new blood vessels in the hemangioma (13). The potential underlying molecular mechanisms include vascular endothelial growth factor (VEGF) and receptors (VEGFR) (14), angiogenin and receptors (15), the Notch signaling pathway (16), mammalian target of rapamycin (mTOR) signaling pathway (17), β-adrenergic receptors and the renin-angiotensin system (18), among others.

Artesunate is an important derivative of artemisinin, and its metabolite dihydro-artemisinin has been used to treat malaria (19). In recent years, studies have identified that artesunate has anti-tumor potential (20). Artesunate has a variety of mechanisms as an anti-tumor agent: It can influence tumor cell apoptosis, the iron-mediated formation of free radicals, anti-angiogenesis, block the cell cycle, anti-immunosuppressive (21), reverse drug resistance and restore chemosensitivity (22,23). A large number of studies are underway, evaluating the anti-cancer activity of artemisinin derivatives; however, artesunate has not yet been studied for hemangioma.

The aim of the current experiment was to explore the effect of artesunate on hemangioma. Thus, EOMA cells were used in an established hemangioma nude mouse model (24,25). Subsequently, the mechanisms of the artesunate-mediated inhibition of EOMA cell proliferation and invasion *in vitro*, and of hemangioma growth *in vivo*, were investigated.

Materials and methods

Antibodies and main reagents. Hypoxia-inducible factor (HIF-1α; cat. no. ab82832), caspase-3 (cat. no. ab13847), VEGFR1 (cat. no. ab32152) and β-actin (cat. no. ab8227) were purchased from Abcam (Cambridge, UK). VEGF-A (cat. no. 31274-1) and VEGFR-2 (cat. no. 21079-1) were purchased from Signalway Antibody LLC., (College Park, Maryland, USA). The EOMA cell line was purchased from the American Type Culture Collection, (ATCC, Manassas, VA, USA). Fetal calf serum (FCS) and Dulbecco's Modified Eagle's Medium (DMEM) were purchased from Gibco (Thermo Fisher Scientific, Inc., Waltham, MA, USA); artesunate was purchased from Guilin Pharmaceutical Co. Ltd., (Guilin, China); MTT was purchased from Sigma-Aldrich (Merck KGaA, Darmstadt, Germany). Matrigel-coated Transwell chambers were purchased from Qiagen GmbH (Hilden, Germany). Apoptosis kits, including propidium iodide (PI) and fluorescein isothiocyanate (FITC)-Annexin V work solution, were purchased from Thermo Fisher Scientific, Inc. PrimeScript™ RT reagent kit with gDNA Eraser and SYBR® Premix Ex Taq™ II were purchased from Takara Bio, Inc., (Otsu, Japan). TRIzol Reagent was purchased from Invitrogen; Thermo Fisher Scientific, Inc.

Cell culture. Cells were cultured in DMEM supplemented with 10% FCS and incubated at 37˚C with 5% CO_2, prior to being used at the logarithmic growth phase.

Growth inhibition assay. An MTT assay was used to assess cell proliferation. The EOMA cells ($1x10^5$/ml) were seeded onto 96-well plates. Artesunate was diluted in 1 ml 5% sodium bicarbonate solution, shaken for 2-3 min producing 0, 100, 200, 300, 400 and 500 μg/ml concentrations and then 100 μl was added to the EOMA cells in each well. At 0, 24, 48 and 72 h, an equal volume of MTT solution was added to each well and cultured for another 4 h. The incubation conditions in this assay were all 37˚C in an atmosphere containing 5% CO_2. MTT-treated cells were fixed with 150 μl dimethyl sulfoxide for 30 min at room temperature and then assayed with an Evolution™ 201/220 UV-Vis spectrophotometer at 490 nm.

Apoptosis assessment. After 24 and 48 h, artesunate-treated (300 μg/ml) cells were collected and washed with cold PBS. Stained cells were assessed with a FACSCalibur™ flow cytometer and analyzed using BD CellQuest™ software (version 5.1; BD Biosciences, Franklin Lakes, NJ, USA). The percentage of early apoptotic cells (stained with Annexin V only) and late apoptotic cells (stained with Annexin V and PI) was recorded. Furthermore, Hoechst 33342 staining solution was used to identify the apoptotic cells, and later detected with fluorescence microscopy. Unstained cells were included as the control.

Transwell invasion assay. A Transwell assay was performed by using Matrigel-coated Transwell chambers (pore size of 8.0 μm). A total of $1x10^5$ cells were re-suspended in 200 μl serum-free medium and seeded into the upper compartment of the chamber. The lower compartment was loaded with 800 μl DMEM containing 10% FCS. After incubation at 37˚C for 36 h, the membranes were fixed with formaldehyde at room temperature for 5 min, and counter-stained with DAPI at room temperature for 30 min in the dark. The staining was examined under a vertical fluorescence microscope. Trans-membrane migrated cells from each sample were counted in three random fields at x200 magnification. The assay was performed in triplicate.

Reverse transcription-quantitative polymerase chain reaction (RT-qPCR) assay. An RT-qPCR assay was used for the quantitative estimation of the mRNA expression of VEGF-A, VEGFR-1, VEGFR-2 and HIF-1α in EOMA cells, in the artesunate and in the control groups. Total RNA from ~$1x10^7$ cells was extracted using TRIzol® reagent, according to the manufacturer's protocol. Total RNA then underwent RT using the PrimeScript™ RT reagent kit with gDNA Eraser. The expression of VEGF-A, VEGFR-1, VEGFR-2 and HIF-1α mRNA was determined using the CFX96 Real-Time Detection System (Bio-Rad Laboratories, Inc., Hercules, CA, USA) using SYBR® Premix Ex Taq™ II. β-actin was used as the internal reference. Data were analyzed using the $2^{-\Delta\Delta Cq}$ method (26). Three separate experiments were performed for each clone. Primers used for PCR analysis were as follows: VEGF-A forward, 5'-CAG GCTGCTGTAACGATGAA-3' and reverse, 5'-TTTCTTGCG CTTTCGTTTTT-3'; VEGFR-1 forward, 5'-GAGGAGGAT GAGGGTGTCTATAGGT-3' and reverse, 5'-GTGATCAGC TCCAGGTTTGACTT-3'; VEGFR-2 forward, 5'-TTCTGG ACTCTCCCTGCCTA-3' and reverse, 5'-AAGGACCATCCC ACTGTCTG-3'; HIF-1α forward, 5'-TGAGCTTGCTCATCA GTTGC-3' and reverse, 5'-CCATCTGTGCCTTCATCTCA-3'; β-actin forward, 5'-AAGATGACCCAGATCATGTTTGAG ACC-3' and reverse, 5'-GCCAGGTCCAGACGCAGGAT-3'.

Western blot analysis. EOMA cells were treated with 300 μg/ml artesunate for 24, 48 and 72 h, washed with cold PBS, harvested and extracted using lysis buffer. The protein concentration was detected using a NanoDrop Lite spectrophotometer (Thermo Fisher Scientific, Inc.). A total of 100 μg protein were separated using SDS-PAGE (10% gel) and then transferred to polyvinylidene fluoride membranes. To eliminate background disturbance, membranes were blocked by incubation in blocking solution (5% low fat milk and 0.1% Tween 20 in TBS) at room temperature for 1 h. Cells were then incubated with a rabbit monoclonal primary antibody specific for VEGF-A (dilution, 1:500), VEGFR-1 (dilution, 1:1,000), VEGFR-2 (dilution, 1:500), HIF-1α (dilution, 1:1,000), caspase-3 (dilution, 1:500) and β-actin (dilution, 1:2,000) at 4˚C overnight, followed by incubation with a secondary antibody for 1 h at room temperature. Following this, enhanced chemiluminescence protein analysis was performed.

Animals. To observe efficacy of intra-tumor injection of artesunate for mouse K-MS and later a comparison with pingyangmycin (PYM), a total of 20 five-week-old female BALB/c nude mice (weight, between 18 and 20 g) were obtained from Chongqing Medical University (Chongqing, China). The mice were housed under specific pathogen-free conditions in an animal facility with free access to pelleted regular rodent diet (Experimental Animal Centre of the Children's Hospital of Chongqing Medical University, Chongqing, China) and water *ad libitum*. The room temperature was between 22-25˚C,

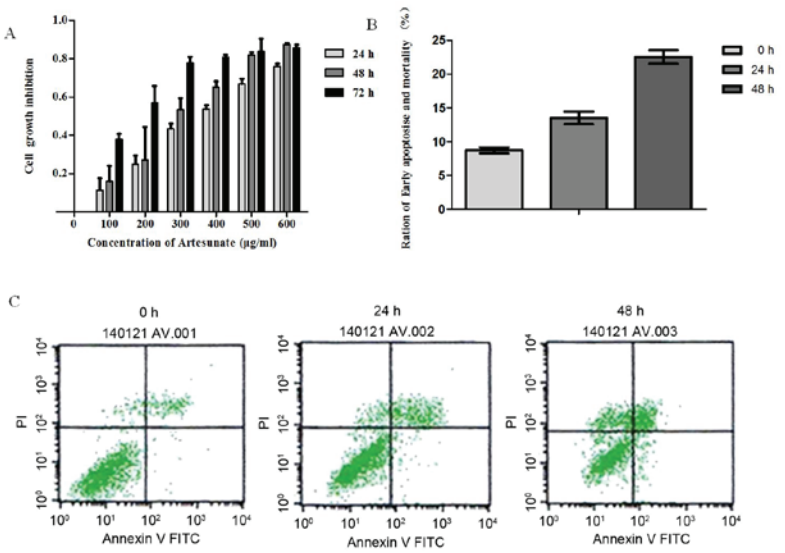

Figure 1. Effect of artesunate on the rate of EOMA cell growth inhibition and the induction of apoptosis in artesunate-treated EOMA cells. (A) Growth inhibition was determined using the MTT assay. Cells were treated with various concentrations of artesunate for the indicated times. The IC_{50} value of artesunate in EOMA cells was 300 μg/ml. The growth of EOMA cells was significantly inhibited by artesunate in a dose- and time-dependent manner. Results presented are the representative data of at least three independent experiments. (B) Annexin V/PI binding assay analysis of apoptosis in artesunate treated EOMA cells lines. The percentages of early apoptosis (Annexin V+/PI-, LR) are depicted. The results are expressed as mean ± standard deviation from three independent experiments (24 h, $P<0.05$ vs. 0 h; 48 h, $P<0.01$ vs. 0 h). (C) Representative images of the respective treatments in the Annexin V/PI binding assay. Results presented are representative data of at least three independent experiments. PI, propidium iodide; FITC, fluorescein isothiocyanate.

humidity was between 45-55%, and a 12-h light-dark diurnal cycle (lights on from 7:00 to 19:00) was used. The Experimental Animal Centre of Children's Hospital of Chongqing Medical University approved the experimental protocols. All procedures were carried out according to the Institutional Animal Care and Use Committee Guide in Child Development and Disorders' Laboratories (Chongqing, China; license no. SYXK (YU)2012-0001; sydwzx.cqmu.edu.cn).

An inoculation of $1x10^7$ EOMA cells in 100 μl PBS was injected into the subcutaneous tissues of the right flank of the female nude mice. The female nude mice were randomly divided into the following four groups of five each: Artesunate group, PYM group, PBS group and no treatment group. Tumor-bearing mice were treated with intra-tumoral injections every three days until the tumor was visible to the naked eye. The PBS group (intra-tumoral injection with the same dose of PBS every three days) was used as the negative control group and the no treatment group (tumor growth was not modified) was considered as the blank control group. As PYM is typically used as a treatment modality for hemangioendothelioma, the curative effect of artesunate was compared with that of PYM. The tumors were measured on alternate days using tissue calipers. Tumor volume was determined using the following formula: $(Width)^2x$ length x0.52. Mice were sacrificed by cervical dislocation when difficulty with ambulation and lethargy had set in.

Statistical analysis. SPSS 13.0 software was used for all data analysis (SPSS, Inc., Chicago, IL, USA). Numerical data are represented as the mean ± standard deviation. Differences between the control and treated groups were determined using the Student's t-test and one-way analysis of variance. Each experiment was performed in triplicate and $P<0.05$ was considered to indicate a statistically significant difference.

Results

Effect of artesunate on the proliferation of EOMA cells. Artesunate treatment significantly inhibited the growth of EOMA cells in a time- and dose-dependent manner (Fig. 1A). The inhibition of cell proliferation increased correspondingly with the increase in drug concentration during the same time. Also, on extension of exposure time, there was an increase in cell proliferation inhibition with the same concentration. However, this inhibitory effect became apparent as ≤50% (IC_{50}) at a concentration of 300 μg/ml artesunate; therefore, this concentration was used throughout the study.

Effect of artesunate on the apoptosis of EOMA cells. Based on the results of the MTT assay, 300 μg/ml of artesunate was used for determining apoptosis. To elucidate the mechanism by which artesunate exerts its anti-proliferative effect on EOMA cell lines, an Annexin V/PI binding assay was performed. Results demonstrated an increased percentage of early apoptotic cells (Annexin V/PI) after treatment of EOMA cells with 300 μg/ml artesunate for 24 h (24 h, $P<0.05$ vs. 0 h), and this percentage of early apoptotic cells increased significantly following incubation for 48 h (48 h, $P<0.01$ vs. 0 h; Fig. 1B and C). The rate of apoptosis for EOMA cells treated with artesunate increased in a time-dependent manner.

Effect of artesunate on the invasion of EOMA cells. To investigate the inhibitory effect of artesunate on the invasion of EOMA cells *in vitro*. The invasion efficiency of EOMA cells in response to artesunate was tested using a Transwell invasion system. The invasion efficiency was calculated as the number of invaded cells to the control. In the presence of artesunate (300 μg/ml), the number of invaded EOMA cells

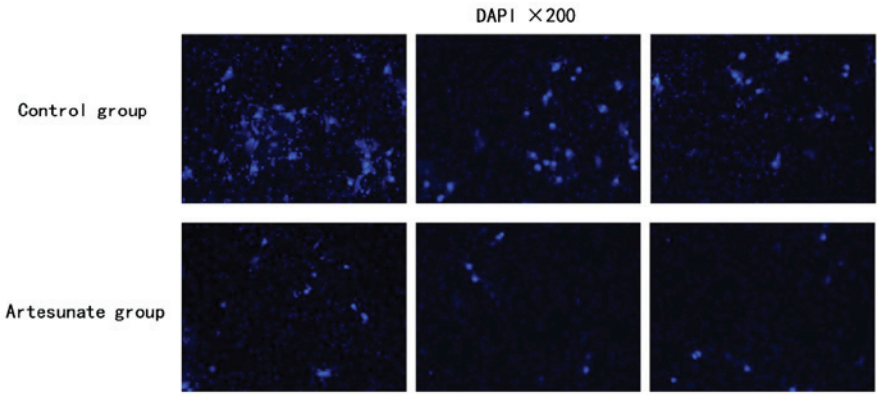

Figure 2. Transwell invasion assay using EOMA cells. The migration efficiency was illustrated as the increase or decrease in the number of invaded cells relative to the control. Cells from each sample were counted in three random fields at x200 magnification (P<0.05). Results presented are representative data of ≥3 independent experiments.

was significantly decreased compared with that of the control group, which has the same number of EOMA cells in the initial stage of this experiment (Fig. 2; P<0.05).

Effect of artesunate on VEGF-A, VEGFR-1, VEGFR-2 and HIF-1α mRNA expression. RT-qPCR was performed to examine the expression of VEGF-A, VEGFR-1, VEGFR-2 and HIF-1α mRNA in EOMA cells treated with artesunate at 300 μg/ml for 24, 48 and 72 h. The results demonstrate that VEGF-A, VEGFR-2 and HIF-1α mRNA expression levels in EOMA cells treated with artesunate were significantly decreased in a time-dependent manner (*P<0.05, $^{\#}$P<0.01; Fig. 3A). There was no statistically significant difference in the VEGFR-1 mRNA expression level among the treatment groups (Fig. 3A).

Effect of artesunate on VEGF-A, VEGFR-1, VEGFR-2, HIF-1 and, caspase-3 protein level. Western blotting was performed to examine the expression of VEGF-A, VEGFR-1, VEGFR-2, HIF-1α and caspase-3 protein in EOMA cells treated with artesunate at 300 μg/ml for 24, 48 and 72 h. The results demonstrated that HIF-1α, VEGF-A and VEGFR-2 protein expression levels in EOMA cells were significantly decreased, but caspase 3 protein expression levels were significantly increased (*P<0.05, $^{\#}$P<0.01; Fig. 3B). There were no statistically significant differences in VEGFR-1 protein expression levels among the treatment groups (Fig. 3C).

Effect of artesunate on the growth of Kasabach-Merritt tumors in nude mice. The outcome of artesunate expression on tumor growth in mice was examined by establishing a subcutaneous K-MS transplantation model. The tumor size was measured every three days (Table I and Fig. 4). The results demonstrated that the volume of the tumor in the artesunate-treated group had significantly reduced, and the effect was approximately equal to that recorded for PYM treatment. Artesunate and PYM can significantly reduce Kasabach-Merritt tumor growth compared with the no treatment and PBS groups (P<0.05). There were no statistically significant differences in tumor size between the artesunate and PYM groups, which was the same between the no treatment and PBS groups (P>0.05).

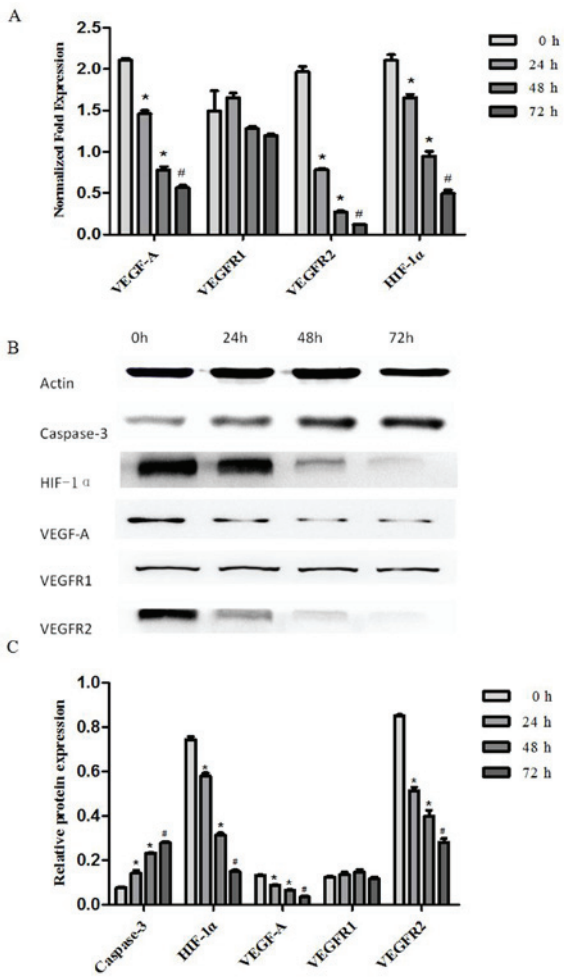

Figure 3. Artesunate suppressed the gene and protein expression of VEGF-A, VEGFR-2 and HIF-1α, and increased the protein expression of caspase-3 in mouse EOMA cell lines. (A) The transcript levels of VEGF-A, VEGFR-1, VEGFR-2 and HIF-1α mRNA were analyzed using RT-qPCR; β-actin was included as the loading control. VEGF-A, VEGFR-2 and HIF-1α expression was significantly downregulated by artesunate. The results are expressed as the mean ± standard deviation from three separate experiments (*P<0.05, $^{\#}$P<0.01, vs. control). (B) Western blot analysis of the protein expression in EOMA cells treated with artesunate for 24, 48 and 72 h, to evaluate VEGFA, VEGFR-1, VEGFR2, HIF-1α and caspase 3 expression. (C) Results presented are representative data of at least three independent experiments (*P<0.05, $^{\#}$P<0.01, vs. control). VEGFR, vascular endothelial growth factor receptor; HIF-1α, hypoxia inducible factor-1α.

Table I. The volume of tumor in every group at various times (mm^3; n=5, mean ± standard error of the mean).

Time	No treatment group	PBS group	PYM group	Artesunate group
0 day	68.9±19.5	80.0±21.2	132.6±23.7	122.4±15.2
3 days	215.3±145.4	161.9±90.4	32.6±79.9	71.4±13.2
6 days	284.9±190.1	241.5±138.4	87.1±213.4	44.4±12.7
9 days	274.3±199.5	492.3±225.1	391.6±161.2	57.4±25.1
12 days	575.8±418.1	751.8±370.9	323.7±135.4	111.1±45.3
15 days	900.3±637.5	1,129.4±319.4	273.9±119.9	139.8±43.0
18 days	1,489.7±1,018.6	1,442.2±604.2	202.2±61.6	167.3±62.9
21 days	1,728.7±975.7	1,559.1±718.2	161.4±58.8	186.8±60.9
24 days	2,165.8±1,041.8	1,819.0±789.3	136.3±58.9	183.4±61.6
27 days	3,163.8±1,688.2	2,033.3±1,021.8	105.6±50.9	184.1±64.3
30 days	3,445.7±1,889.8	2,337.4±1,282.7	84.1±33.3	188.6±61.5

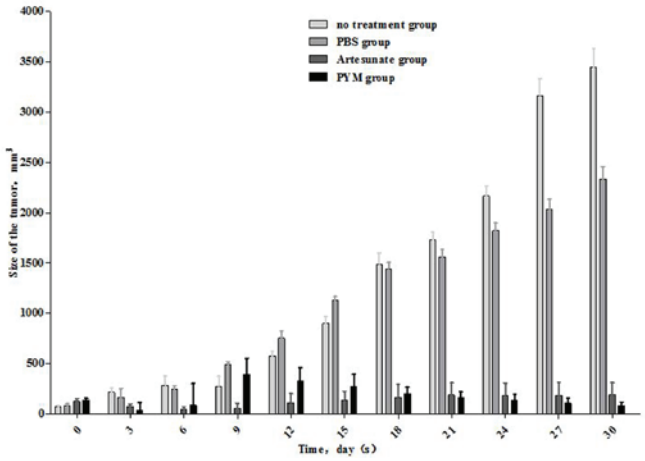

Figure 4. Artesunate, PYM and PBS were used to establish Kasabach-Merritt tumors in nude mice. Tumor size was monitored for 30 days. Artesunate depressed tumor growth, as compared with PYM group (P>0.05), and as compared with the no treatment and PBS groups (P<0.05).

Discussion

K-MS is a life-threatening complication of hemangioma; its most common histological appearance is as Kaposiform hemangioendothelioma (46% cases), followed by plexiform vascular (31%) and capillary tumors (23%) (27). The primary clinical manifestations are a rapid increase in tumor size, progressive decrease in platelet count, microvascular anemia, blood coagulation dysfunction and serious internal bleeding (28). EOMA cells were originally derived from 129/J mice spontaneous hemangioendothelioma (29). *In vitro*, EOMA cells exhibit the typical characteristics of the endothelial cells; these can grow in the matrix with tubular structure rearrangement and their biological actions are similar to those of microvascular endothelial cells (30). Studies have identified that EOMA cells administered to 129/J mice subcutaneously or nude mice can form histological and hematological characteristics similar to hemangioma with a K-MS animal model (24,25). EOMA cells have been demonstrated to be useful in constructing K-MS models with high rates of quick forming tumors; therefore, EOMA cells are widely used for the study of angiogenesis inhibitors (31).

A number of positive and negative regulators control the angiogenic process, particularly the VEGF family and angiopoietins (32). VEGF-A is one of the most potent angiogenic factors, which induces migration and proliferation in endothelial cells, correlates with vascular density and influences prognosis (33). VEGFR-1 and VEGFR-2 are VEGFA receptors that mediate numerous biological activities, including: Proliferation, migration, tyrosine phosphorylation of downstream targets, Ca^{2+} mobilization, prostacyclin production, extracellular signal regulated kinase activation, nitric oxide production and phosphatidylinositol-3-kinase/protein kinase B activity (34). Hypoxia can induce the expression of HIF-1 and HIF-2, which may then upregulate the transcription factors for VEGF (35). Thus, VEGF secretes under hypoxic conditions and binds to its receptors, which are located on the surface of vascular endothelial cells (36). Hypoxic conditions can upregulate the expression of VEGF, while tissues can increase their oxygenation in order to induce blood vessel growth (37). By contrast, normoxia downregulates the expression of VEGF and can degenerate newly formed blood vessels (38). The vasculature exactly satisfies the metabolic requirements of the tissue through these opposing processes (39). Though hemodynamic forces, such as shear stress, are fundamental for remodeling, tissue hypoxia appears to serve an essential role in the coordinated expression of all angiogenic factors. Once oxygenation has reached normal levels, they are rapidly downregulated and HIF levels decrease (40).

Various treatment modalities are available for K-MS, the commonly used drugs including triamcinolone acetate and PYM (41,42). A disadvantage is that the long-term adverse effects are problematic to assess and the mechanism of action is also unclear. Another study has identified that rapamycin acts by inhibiting the mTOR pathway, thus suppressing HIF-1α and VEGF and subsequently inhibiting vascular endothelial cell proliferation (43). A study also identified that propranolol decreases HIF-1α, reduces downstream VEGF, VEGFR-1 and VEGFR-2 and the expression of monocyte chemoattractant protein-1, thus inhibiting angiomatous proliferation; however,

there were no significant differences in the expression of matrix metalloproteinases (44).

Artesunate, a compound isolated from a traditional Chinese medicine plant, is currently being evaluated for anti-tumor activity (45,46). Chinese medicine workers first identified artemisinin in the early 1970s as an effective antimalarial ingredient, extracted from sweet wormwood (*Artemisia annua*) (47). The history of artemisinin drugs used in the clinical treatment of malaria is decades old, thus it has become a well-established clinical drug and no severe systemic or local adverse drug reactions have been identified to date (48). With the development of scientific technology, the understanding of pharmaceutical ingredients present in traditional Chinese medicine has increased, and the pharmacological effects of the effective components are under further study (49).

Targeting angiogenesis is one of the treatment modalities in cancer management (50-52). Dihydro-artemisinin can decrease the expression of VEGF, inhibit the formation of new blood vessels and promote the apoptosis of tumor cells in leukemia cell line K562 animal models (53). Studies have identified that artemisinin has inhibitory effect on A549 human lung adenocarcinoma cells, and that its mechanism of action may be to inhibit cell proliferation, induce apoptosis and cell cycle arrest (54,55). Thus, the co-administration of artemisinin derivatives with other anti-cancer agents may increase the concentration of those anti-cancer drugs in the cell (56). In the present study, it was identified that artesunate can inhibit the proliferation, apoptosis and invasion of EOMA cells *in vitro* by reducing the expression of HIF-1α, VEGF-A and VEGFR-2. It was also determined that artesunate can inhibit the growth of a vascular tumor *in vivo*, with a curative effect similar to that of PYM.

In conclusion, the traditionally used anti-malarial drug artesunate has a significant inhibitory effect on hemangioma growth. This property should be evaluated further and may become a potential treatment option for hemangioma, with the advantages of fewer toxic side effects and higher cost-efficiency.

Acknowledgements

This project was supported by the National Natural Science Foundation of China (grant no. 30973136) and the Project of Children's Hospital of Chongqing Medical University (grant no. 7000003).

References

1. Bruckner AL and VFrieden IJ: Hemangiomas of infancy. J Am Acad Dennatol 48: 477-496, 2003.
2. Xu D, O TM, Shartava A, Fowles TC, Yang J, Fink LM, Ward DC, Mihm MC, Waner M and Ma Y: Isolation, characterization, and in vitro propagation of infantile hemangioma stem cells and an in vivo mouse model. J Hematol Oncol 4: 54, 2011.
3. Yasui N, Koh K, Kato M, Park MJ, Tomizawa D, Oshima K, Uchisaka N, Gocho Y, Arakawa A, Seki M, *et al*: Kasabach-Merritt phenomenon: A report of 11 cases from a single institution. J Pediatr Hematol Oncol 35: 554-558, 2013.
4. Fernandez-Pineda I, Lopez-Gutierrez JC, Chocarro G, Bernabeu-Wittel J and Ramirez-Villar GL: Long-term outcome of vincristine-aspirin-ticlopidine (VAT) therapy for vascular tumors associated with Kasabach-Merritt phenomenon. Pediatr Blood Cancer 60: 1478-1481, 2013.
5. O'Regan GM, Irvine AD, Yao N, O'Marcaigh A, Sheridan-Pereira M, Phelan E, McDermott MB, Twomey A, Russell J and Watson R: Mediastinal and neck kaposiform hemangioendothelioma: Report of three cases. Pediatr Dermatol 26: 331-337, 2009.
6. Sarkar M, Mulliken JB, Kozakewich HP, Robertson RL and Burrows PE: Thrombocytopenic coagulopathy (Kasabach-Merritt phenomenon) is associated with kaposiform hemangioendothelioma and not with common infantile hemangioma. Plast Reconstr Surg 100: 1377-1386, 1997.
7. Wang Z, Li K, Yao W, Dong K, Xiao X and Zheng S: Steroid-resistant kaposiform hemangioendothelioma: A retrospective study of 37 patients treated with vincristine and long-term follow-up. Pediatr Blood Cancer 62: 577-580, 2015.
8. Enjolras O, Wassef M, Mazoyer E, Frieden IJ, Rieu PN, Drouet L, Taïeb A, Stalder JF and Escande JP: Infants with Kasabach-Merritt syndrome do not have 'true' hemangiomas. J Pediatr 130: 631-640, 1997.
9. Cooper JG, Edwards SL and Holmes JD: Kaposiform haemangioendothelioma: Case report and review of the literature. Br J Plast Surg 55: 163-165, 2002.
10. Enjolras O, Mulliken JB, Wassef M, Frieden IJ, Rieu PN, Burrows PE, Salhi A, Léauté-Labreze C and Kozakewich HP: Residual lesions after Kasabach-Merritt phenomenon in 41 patients. J Am Acad Dermatol 42: 225-235, 2000.
11. Hervella M and Iqlesias ME: Vascular tumors as syndromic indicators. An Sist Sanit Navar 27 (Suppl 1): S33-S44, 2004 (In Spanish).
12. Haisley-Royster C, Enjolras O, Frieden IJ, Garzon M, Lee M, Oranje A, de Laat PC, Madern GC, Gonzalez F, Frangoul H, *et al*: Kasabach-Merritt phenomenon: A retrospective study of treatment with vincristine. J Pediatr Hematol/Oncol 24: 459-462, 2002.
13. Greenberger S and Bisehoff J: Pathogenesis of infantile haemangioma. Br J Dermatol 169: 12-19, 2013.
14. Przewratil P, Sitkiewicz A and Andrzejewska E: Local serum levels of vascular endothelial growth factor in infantile hemangioma: Intriguing mechanism of endothelial growth. Cytokine 49: 141-147, 2010.
15. Koh GY: Orchestral actions of angiopoietin-1 in vascular regeneration. Trends Mol Med 19: 31-39, 2013.
16. Phng LK and Gerhardt H: Angiogenesis: A team effort coordinated by notch. Dev Cell 16:196-208, 2009.
17. Laplante M and Sabatini DM: mTOR signaling in growth control and disease. Cell 149: 274-293, 2012.
18. Léauté-Labrèze C, Dumas de la Roque E, Hubiche T, Boralevi F, Thambo JB and Taïeb A: Propranolol for severe hemangiomas of infancy. N Engl J Med 358: 2649-2651, 2008.
19. Sagara I, Beavogui AH, Zongo I, Soulama I, Borghini-Fuhrer I, Fofana B, Camara D, Somé AF, Coulibaly AS, Traore OB, *et al*: Safety and efficacy of re-treatments with pyronaridine-artesunate in African patients with malaria: A sub study of the WANECAM randomised trial. Lancet Infect Dis 16: 189-198, 2016.
20. Efferth T, Li PC, Konkimalla VS and Kaina B: From traditional Chinese medicine to rational cancer therapy. Trends Mol Med 13: 353-361, 2007.
21. Zhang LX, Liu ZN, Ye J, Sha M, Qian H, Bu XH, Luan ZY, Xu XL, Huang AH, Yuan DL, *et al*: Artesunate exerts an anti-immunosuppressive effect on cervical cancer by inhibiting PGE2 production and Foxp3 expression. Cell Biol Int 38: 639-646, 2014.
22. Jeong DE, Song HJ, Lim S, Lee SJ, Lim JE, Nam DH, Joo KM, Jeong BC, Jeon SS, Choi HY and Lee HW: Repurposing the anti-malarial drug artesunate as a novel therapeutic agent for metastatic renal cell carcinoma due to its attenuation of tumor growth, metastasis, and angiogenesis. Oncotarget 6: 33046-33064, 2015.
23. Mukanganyama S, Naik YS, Widersten M, Mannervik B, Hasler JA: Proposed reductive metabolism of artemisinin by glutathione transferases in vitro. Free Radic Res 35: 427-434, 2001.
24. Wang C, Quevedo ME, Lannutti BJ, Gordon KB, Guo D, Sun W and Paller AS: In vivo gene therapy with interleukin-12 inhibits primary vascular tumor growth and induces apoptosis in a mouse model. J Invest Dermatol 112: 775-781, 1999.
25. Sidbury R, Neuschler N, Neuschler E, Sun P, Wang XQ, Miller R, Tomai M, Puscasiu E, Gugneja S and Paller AS: Topically applied imiquimod inhibits vascular tumor growth in vivo. J Invest Dermatol 121: 1205-1209, 2003.
26. Livak KJ and Schmittgen TD: Analysis of relative gene expression data using real-time quantitative PCR and the 2(-Delta Delta C(T)) method. Methods 25: 402-408, 2001.

27. Alvarez-Mendoza A, Lourdes TS, Ridaura-Sanz C and Ruiz-Maldonado R: Histopathology of vascular lesions found in Kasahach-Merritt syndrome: Review based on 13 cases. Pediatr Dev Pathol 3: 556-560, 2000.
28. Hammill AM, Wentzel M, Gupta A, Nelson S, Lucky A, Elluru R, Dasgupta R, Azizkhan RG and Adams DM: Sirolimus for the treatment of complicated vascular anomalies in children. Pediatr Blood Cancer 57: 1018-1024, 2011.
29. Gordillo GM, Atalay M, Roy S and Sen CK: Hemangioma model for in vivo angiogenesis: Inducible oxidative stress and MCP-1 expression in EOMA cells. Methods Enzymol 352: 422-432, 2002.
30. Lannutti BJ, Gately ST, Quevedo ME, Soff GA and Paller AS: Human angiostatin inhibits murine hemangioendothelioma tumor growth in vivo. Cancer Res 57: 5277-5280, 1997.
31. O'Reilly MS, Brem H and Folkman J: Treatment of murine hemangioendotheliomas with the angiogenesis inhibitor AGM-1470. J Pediatr Surg 30: 325-330, 1995.
32. Breier G, Albrecht U, Sterrer S and Risau W: Expression of vascular endothelial growth factor during embryonic angiogenesis and endothelial cell differentiation. Development 114: 521-532, 1992.
33. O'Reilly MS, Holmgren L, Shing Y, Chen C, Rosenthal RA, Moses M, Lane WS, Cao Y, Sage EH and Folkman J: Angiostatin: A novel angiogenesis inhibitor that mediates the suppression of metastases by a Lewis lung carcinoma. Cell 79: 315-328, 1994.
34. O'Reilly MS, Boehm T, Shing Y, Fukai N, Vasios G, Lane WS, Flynn E, Birkhead JR, Olsen BR and Folkman J: Endostatin: An endogenous inhibitor of angiogenesis and tumor growth. Cell 88: 277-285, 1997.
35. Dvorak HF, Brown LF, Detmar M and Dvorak AM: Vascular permeability factor/vascular endothelial growth factor, microvascular hyperpermeability, and angiogenesis. Am J Pathol 146: 1029-1039, 1995.
36. Olsson AK, Dimberg A, Kreuger J and Claesson-Welsh L: VEGF receptor signalling-in control of vascular function. Nat Rev Mol Cell Biol 7: 359-371, 2006.
37. Manalo DJ, Rowan A, Lavoie T, Natarajan L, Kelly BD, Ye SQ, Garcia JG and Semenza GL: Transcriptional regulation of vascular endothelial cell responses to hypoxia by HIF-1. Blood 105: 659-669, 2005.
38. Ferrara N, Gerber HP and LeCouter J: The biology of VEGF and its receptors. Nat Med 9: 669-676, 2003.
39. Jain RK: Molecular regulation of vessel maturation. Nat Med 9: 685-693, 2003.
40. Iruela-Arispe ML and Dvorak HF: Angiogenesis: A dynamic balance of stimulators and inhibitors. Thromb Haemost 78: 672-677, 1997.
41. Chowdri NA, Darzi MA, Fazili Z and Iqbal S: Intralesional corticosteroid therapy for childhood cutaneous hemangiomas. Ann Plast Surg 33: 46-51, 1994.
42. Cao X, He N, Sun J, Wang S, Ji X, Wang J, Zhang C, Yang J, Lu T, Li J and Zhang G: Interventional treatment of huge hepatic cavernous hemangioma. Chin Med J (Engl) 113: 927-929, 2000.
43. Medici D and Olsen BR: Rapamycin inhibits proliferation of hemangioma endothelial cells by reducing HIF-1-dependent expression of VEGF. PLoS One 7: e42913, 2012.
44. Chim H, Armijo BS, Miller E, Gliniak C, Serret MA and Gosain AK: Propranolol induces regression of hemangioma cells through HIF-1α-mediated inhibition of VEGF-A. Ann Surg 256: 146-156, 2012.
45. Yang ND, Tan SH, Ng S, Shi Y, Zhou J, Tan KS, Wong WS and Shen HM: Artesunate induces cell death in human cancer cells via enhancing lysosomal function and lysosomal degradation of ferritin. J Biol Chem 289: 33425-33441, 2014.
46. Efferth T, Dunstan H, Sauerbrey A, Miyachi H and Chitambar CR: The anti-malarial artesunate is also active against cancer. Int J Oncol 18: 767-773, 2001.
47. Chemical studies on qinghaosu (artemisinine). China cooperative research group on qinghaosu and its derivatives as antimalarials. J Tradit Chin Med 2: 3-8, 1982.
48. Douglas NM, Anstey NM, Angus BJ, Nosten F and Price RN: Artemisinin combination therapy for vivax malaria. Lancet Infect Dis 10: 405-416, 2010.
49. Chan K: Chinese medicinal materials and their interface with Western medical concepts. J Ethnopharmacol 96: 1-18, 2005.
50. Hanahan D and Weinberg RA: Hallmarks of cancer: The next generation. Cell 144: 646-674, 2011.
51. Aggarwal C, Somaiah N and Simon G: Antiangiogenic agents in the management of non-small cell lung cancer: Where do we stand now and where are we headed? Cancer Biol Ther 13: 247-263, 2012.
52. Imai K and Takaoka A: Comparing antibody and small-molecule therapies for cancer. Nat Rev Cancer 6: 714-727, 2006.
53. Zhou HJ, Wang WQ, Wu GD, Lee J and Li A: Artesunate inhibits angiogenesis and downregulates vascular endothelial growth factor expression in chronic myeloid leukemia K562 cells. Vascul Pharmacol 47: 131-138, 2007.
54. Liao K, Li J and Wang Z: Dihydroartemisinin inhibits cell proliferation via AKT/GSK3β/cyclinD1 pathway and induces apoptosis in A549 lung cancer cells. Int J Clin Exp Pathol 7: 8684-8691, 2014.
55. Tong Y, Liu Y, Zheng H, Zheng L, Liu W, Wu J, Ou R, Zhang G, Li F, Hu M, *et al*: Artemisinin and its derivatives can significantly inhibit lung tumorigenesis and tumor metastasis through Wnt/β-catenin signaling. Oncotarget 7: 31413-31428, 2016.
56. Ma H, Yao Q, Zhang AM, Lin S, Wang XX, Wu L, Sun JG and Chen ZT: The effects of artesunate on the expression of EGFR and ABCG2 in A549 human lung cancer cells and a xenograft model. Molecules 16: 10556-10569, 2011.